Changes in fire regimes on the Chinese Loess Plateau since the last glacial maximum and implications for linkages to paleoclimate and past human activity

Xu Wang [a,*], Zhongli Ding [a], Ping'an Peng [b]

[a] Key Laboratory of Cenozoic Geology and Environment, Institute of Geology and Geophysics, Chinese Academy of Sciences, P.O. Box 9825, Beijing, 100029, China
[b] Guangzhou Institute of Geochemistry, Chinese Academy of Sciences, P.O. Box 1131, Guangzhou, 510640, China

A B S T R A C T

A high-resolution black carbon (BC) record from 27.5 kyr BP to present was reconstructed using a chemical oxidation method on loess and paleosol samples from the Lijiayuan section of the Chinese Loess Plateau. The black carbon mass sedimentation rates (BCMSR) and carbon isotopic record reveal a paleofire history and its relationship with climate and vegetation changes at the study site. The BCMSR record was decomposed into two components: background BCMSR and the BCMSR peaks. The background BCMSR represents regional fires and shows high fire activities occurred contemporaneous with the Younger Dryas, Older Dryas, Heinrich events and Greenland stadials as registered in the loess grain size record. This suggests a rapid response of regional fires on the Loess Plateau to abrupt climate changes. Spectral analysis of background BCMSR showed two meaningful periodicities of 1620 and 1040 years, close to the cyclicity of the East Asian monsoon as recorded in the stalagmite $\delta^{18}O$ record in Central China. This indicates a tight control of millennial scale wet–dry changes in the monsoonal climate on regional fires on the Loess Plateau. By contrast, the BCMSR peaks are considered to reflect local fire episodes. The occurrences of local fires were more frequent during the last glacial period, with a maximum frequency of ~6 episodes/1000 years during the Last Glacial Maximum (LGM) (22.3 to 14.6 kyr BP), when the climate was drier and more continuous grassy fuels existed on the landscape. During the last glacial–interglacial transition (LGIT) period (14.6 to 11.0 kyr BP), fire frequency was largely reduced due to an increase in precipitation and more woody vegetation. If the LGIT period is taken as an analog for the projected near future, then future global warming alone may not produce large wildfires in northwestern China. Wildfires remained infrequent during the early-to-middle Holocene. Biomass burning increased after 4.0 kyr BP, when the climate became drier and land-use was more intensive. BC carbon isotope ratios may well reflect changes in the vegetation being burnt (i.e., grasses versus trees), yielding results consistent with the associated pollen data in the region.

© 2011 Elsevier B.V. All rights reserved.

1. Introduction

Large frequent fires have been linked to anthropogenic climate change (Westerling et al., 2006) and have been projected to become more frequent under future conditions in the U.S. and other parts of the world (e.g., International Panel on Climate Change, 2007; U.S. Climate Change Science Program, 2008). However, the effects of future climate change upon the incidence of fires are still an open question and more research in a diversity of environments, particularly in the Asian monsoonal region of China, is required to provide a more complete picture. Previous work has fostered an increasing effort to study the relations among climate changes, vegetation and fires to predict future changes in fire activities. In addition, the effects of climate on fuel buildup and fire regimes on multiple time scales have recently received much attention since it is important to understand

past controls on fire regimes and this information can help understand present and future conditions (e.g., Swetnam, 1993; Van der Werf et al., 2006; Power et al., 2008; Whitlock et al., 2008). To date, several studies have linked a shift in fire regimes at individual sites and in generalized regions to rapid climate changes (e.g., Clark et al., 1996; Marlon et al., 2009; Vannière et al., 2011). Nevertheless, the lack of empirical data on long-term linkages between climate changes and fire activities in northern China limit our ability to determine vegetation–fire–climate relationships in the past and how these might be useful for projecting future conditions, especially on millennial time scales, where data is minimal (e.g., Li et al., 2005; Tan et al., 2005; Cao et al., 2007). In addition, anthropogenic activities must have affected or even changed the frequency and/or intensity of fires that occurred in the past. However, it is not yet known to what extent this type of influence happened and how the altered fire regimes disturbed the interactions between vegetation and climate. Therefore, studies in this aspect also need to be carried out.

The Chinese loess deposits have been considered as an ideal depositional environment to register natural fire changes (Wang et al.,

2005), due to the completeness and continuity of loess deposition and preservation (Ding et al., 2002). Here we report a detailed record of fire history for the last 27.5 kyr from the Lijiayuan loess–paleosol section in the northwestern part of Chinese Loess Plateau (CLP). The Lijiayuan section was chosen because: one, results of paleoclimate studies (e.g., Ren et al., 1996; Ding et al., 1998a) provide an understanding of climate changes at millennial time scales that have occurred since the last glacial period that can be used to compare with our reconstruction of biomass burning and fire activity; two, human activities in the region can be traced back to neolithic times (Shui, 2001), which will enable us to examine the impacts of human activities on biomass burning through time; and three, Lijiayuan lies in the desert/loess transition zone, the so-called eclogical fragile zone, an area particularly sensitive to climate change (e.g., Zhou et al., 2002). We are particularly interested in the last glacial–interglacial transition. Significant changes in climate and biota occurred worldwide during this time. The paleoenvironmental records from the CLP region suggest major reorganizations in vegetation occurred during rapid events such as the Younger Dryas (YD) Chronozone, the Bølling–Allerød (B/A) period and Dansgaard–Oeschger cycles (D–O cycles) (Zhou et al., 1996, 1999; An, 2000; Li et al., 2006). Such changes provide an opportunity to examine the response of fire regimes to rapidly changing environmental conditions in the region.

In this study, we measured black carbon abundance, using a chemical oxidation pretreatment (Lim and Cachier, 1996), on loess–paleosol to reconstruct fire history, and carbon isotope composition of black carbon to constrain vegetation changes. The term black carbon (BC) is used to describe a relatively inert and ubiquitous form of carbon, comprising a range of materials from char and charcoal to elemental or graphite carbon produced by the incomplete combustion of fossil fuels and biomass (Goldberg, 1985; Schmidt and Noack, 2000). Due to its inertness, BC signatures in geological deposits can be used as evidence of natural fires (Goldberg, 1985; Lim and Cachier, 1996; Schmidt and Noack, 2000; Thevenon et al., 2010). Black carbon mass sedimentation rate (BCMSR) was employed as an indicator of paleofires occurrence, and the δ^{13}C values of BC could elucidate changes in vegetation that were burnt, with the goal of identifying the linkages among fires, vegetation and abrupt climate changes on the Chinese Loess Plateau. Moreover, we also examined the impacts of human activities on biomass burning since the middle Holocene.

2. Study area and loess–paleosol profile

The Lijiayuan section (36°7′0″N, 104°51′30″E) is located to the north of Huining County, Gansu Province in the northwestern part of the Loess Plateau and is ~100 km from the modern desert margin (Fig. 1). At present, the mean annual temperature is ~7 °C at the site, with a July average of 22.6 °C and a January average of −7.7 °C. The mean annual precipitation is ~250 mm, and about 70% of the rainfall occurs in summer, brought by the East Asia summer monsoon (Wang et al., 2005). In winter, the prevailing winds are northwesterly and generate frequent dust storms due to the high pressure over Siberia.

The landscape in this area is semiarid steppe (Chen, 1987). The vegetation is characterized by herbs, shrubs, and deciduous broad-leaved trees. The dominant herbs include *Artemisia*, *Stipa*, *Achnatherum*, *Cleistogenes*, *Typha*, and *Ephedra*, together with such xerophytic herbs as *Peganum* and *Agriophyllum* (Department of Geography, Shaanxi Normal University, 1987). The dominant elements of deciduous broad-leaved trees include *Betula*, *Quercus*, *Salix*, *Ulmus*, and *Alnus*, which only grow on undisturbed loess hills because of a long history of crop planting. Today, natural fires in the region mainly occur in the winter and spring seasons (from October to April) (Li, 2006). The dry weather during this time causes more fuel to buildup, and the strong winds facilitate the desiccation of fuels and also favor the spread of fires over the landscape (Li, 2006; Zhang et al., 2007).

The loess deposits above S1 of the Lijiayuan section have been sampled and analyzed in previous studies (Ren et al., 1996; Ding et al., 1998a, 1998b; Liu and Ding, 1998). Paleosol S1 is correlated to marine oxygen stage 5, 130 kyr BP (Liu, 1985; Kukla, 1987). The Lijiayuan section is situated in a flat, extensive, high tableland. The thickness of the loess–soil sequence above S1 is ~25 m at Lijiayuan (Fig. 2A). The Holocene soil (S0) in the section is 1.8 m thick and is characterized by a dark color, a massive structure, and some white-colored, secondary carbonate pseudomycella. Above this Holocene soil (S0), a thin layer (~0.4 m) of loess (L0) formed during the late Holocene. The thickness of the last glacial loess (L1) is ~16 m at Lijiayuan. The loess horizon is coarse grained and has a dull yellow orange color (10YR7/4 of Munsell color) and a massive structure. The last interglacial soil (S1) is ~6 m thick and is composed of three individual soils and two thin intervening loess horizons (Fig. 2A). The soil shows a brown color (Munsell color: 10YR4/6–7.5YR4/6) and a massive structure. Ren et al. (1996) took samples continuously at ~2 cm intervals and collected a total of about 1300 samples.

The time-scale for the Lijiayuan section was produced using the Earth orbital tuning method (Ren et al., 1996; Ding et al., 1998a, 1998b; Liu and Ding, 1998). The orbital tuning method was initially developed by Imbrie et al. (1984), and recently improved by Ding et al. (1994) and Yu and Ding (1998) for application to loess deposits. To date, it is widely used in the establishment of time scales for loess–paleosol sequences. Based on the time-scale, the median grain size in Lijiayuan can be well correlated with the oxygen isotope record of the GISP2 ice core at Summit in Greenland and Heinrich events recorded in the North Atlantic Ocean (Ren et al., 1996; Ding et al., 1998a, 1998b; Liu and Ding, 1998). The time difference of the climatic events between the record at Lijiayuan and that in Greenland is in general within 1000 years (Ding et al., 1998a; Liu and Ding, 1998). To independently examine the reliability for our time scale, we compared the age model of the Lijiayuan section with radiocarbon dating of organic materials from the loess sequence in the Weinan section (Liu et al., 1994) via matching the grain size profiles between the sections (Fig. 2A). The matching can be made because these two sections are stratigraphically correlative in the field and coeval changes are also observed in the grain size records (Ding et al., 2001; Wang et al., 2005). Results show that two age models correlate very well to each other with less than 1000 years difference (Fig. 2B). The sample spacing (~2 cm) yields a mean depositional resolution of ~50–80 years for the loess unit (L1) and ~100–150 years for the soil unit (S0), allowing for a millennial-scale fire history record.

3. Methods

In this study, we measured both BC abundance and δ^{13}C of BC on the loess and paleosol samples in the section above 7.26 m in depth, spanning the Holocene and late last glacial period. A total of 346 and 84 samples were analyzed for BC abundance (at ~2 cm interval) and δ^{13}C of BC (at ~10 cm interval), respectively.

We used the chemical method developed by Lim and Cachier (1996) to extract the BC in the loess–soil samples. In brief, the carbonates and part of the silicates in the samples were removed by an acid treatment with HCl (3 mol/L) and HF (10 mol/L)/HCl (1 mol/L) in sequence. The treated samples were then oxidized by a solution of 0.1 mol/L $K_2Cr_2O_7$/2 mol/L H_2SO_4 at 55 °C for 60 h to remove soluble organic matter and kerogen. After the treatment, the remaining refractory carbon in the residue is called BC, and includes charcoal and the atmospheric BC particles from regional fires as well as other sources besides fire (Lim and Cachier, 1996). The contents of black carbon in the residues were combusted at 960 °C using a Heraeus CHN-O Rapid elemental analyzer, repeated six times on duplicate samples (sd < ±3%).

δ^{13}C analyses were performed on a continuous-flow isotope ratio mass spectrometer (CF-IRMS). The CF-IRMS system consists of an elemental analyzer (Flash 1112 series) coupled to a Finnigan MAT 253 mass spectrometer. The standard samples with known δ^{13}C value
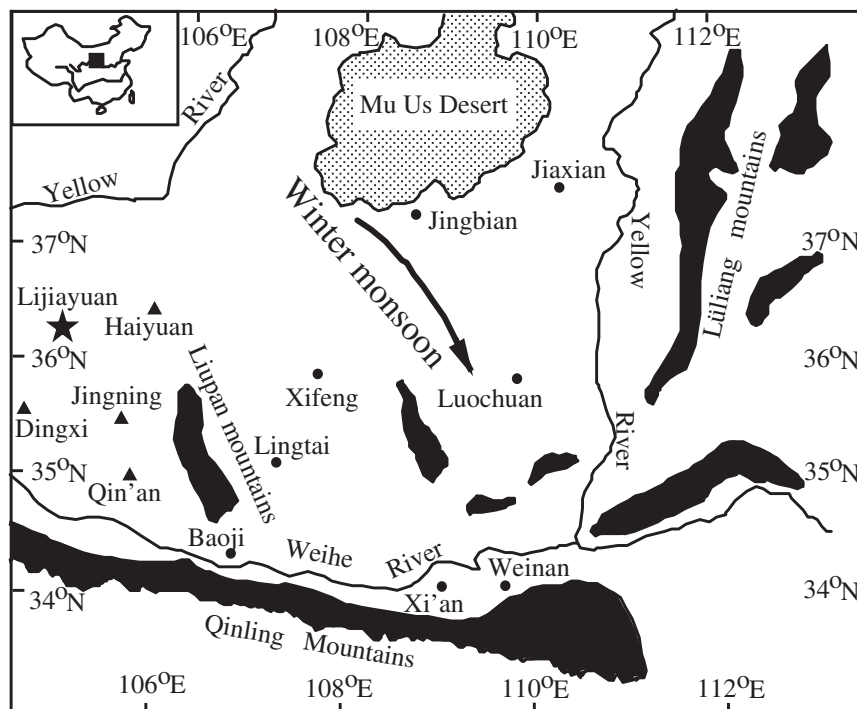
Fig. 1. Location map showing the locality of the studied section labeled as a star. The filled triangles indicate the study sites for pollen data used in this study. The arrow indicates the dominant subaerial wind direction in winter season, coinciding with the observed decrease in grain size and thickness of loess. The desert (dotted area) and mountains (black areas) around and within the Loess Plateau are shown. The solid square in the inset map shows the locality of the Loess Plateau in continental China.

(e.g., Glycine: $\delta^{13}C_{VPDB} = -33.3‰$) were used to monitor the measurement. Analytical precisions were better than $\pm 0.2‰$.

Spectral analysis was conducted on the BCMSR time series using the program REDFIT, which is particularly suitable for estimating red noise spectra directly from unevenly spaced paleoclimatic time series data (Schulz and Mudelsee, 2002). We scaled the theoretical red-noise spectrum by an appropriate percentile of the χ^2-probability distribution to obtain a false-alarm level, which marks the maximum spectral amplitude expected if the time series would have been generated by a first-order autoregressive (AR1) process. Accordingly, spectral peaks exceeding the false-alarm level indicate non-AR1 components in a time series, and should be considered significant. The oversampling factor for Lomb–Scargle Fourier transform (OFAC) was set to 4 and the Max. frequency to analyze (HIFAC) is set to 1. The 1000 Monte-Carlo simulations were used for the bias-correction. Here we adopted the results with a false-alarm level of 90%.

4. Data analysis and interpretation

Data used to reconstruct fires using charcoal preserved in lake sediment cores are typically presented as charcoal accumulation rates (CHAR = area or number of particles/cm^2 per year) (Clark and Royall, 1995a; Whitlock et al., 2003a; Whitlock and Bartlein, 2004). Data analysis methods usually involve a decomposition that detrends a charcoal series and then applies a threshold value to isolate individual peaks (Higuera et al., 2010). Local fire events or episodes (i.e., more than one fire occurring during a given time interval) are inferred from 'peaks' in CHAR. This interpretation is based on assumptions that fire events produce a large number of charcoal particles, and larger (>125 μm) particles generally travel relatively short distances (i.e., within 10^1–10^3 m) before deposition (Clark, 1988; Whitlock and Millspaugh, 1996; Ohlson and Tryterud, 2000). It also assumes that fires consumed enough biomass to produce enough charcoal to register a peak in the lake sediments. Often small fires that produce little charcoal are hard to detect (see Whitlock et al., 2004). CHAR data also display slowly varying trends, referred to as 'background' charcoal

(BCHAR). BCHAR are ascribed to changes in regional fire incidence (Clark and Royall, 1995b) and biomass (Long et al., 1998; Whitlock et al., 2003b), as well as to non-fire-related processes, such as mass-wasting and redeposition (e.g., from lake-level fluctuations; Lynch et al., 2004a), sedimentation rates and bioturbation (Millspaugh and Whitlock, 1995; Carcaillet et al., 2002). Here we use black carbon mass sedimentation rate (BCMSR = number of mg C/cm^2 per year) to reconstruct fire history from the loess–paleosol section (e.g., Wang et al., 2005). The analysis of high-resolution BC records also employs a similar evaluation of "peaks" and BCHAR as described above.

The original BC record was analyzed using the decomposition technique of Long et al. (1998). Concentration values (mg C/cm^3) and deposition times (year/cm) were interpolated into annual values. Annual values were averaged over the interval of 50 years (bins). Binned concentration values were then divided by average deposition times of the binned interval to obtain time series of BC mass sedimentation rates (BCMSR) (mg C/cm^2 per year). BCMSR time series were logarithmically transformed for variance stabilization (Log(BCMSR + 1)) before being decomposed into background and peaks components (Charster software, D.G. Gavin, unpublished data, 2006). A locally-weighted mean was used to estimate the background component of the BCMSR data. The peaks component (or fire episode series) was derived as the positive deviations from a local mean that exceeded a certain threshold value (see Section 5.2 for the selection of threshold value). Here all the positive peaks were considered as signals reflecting discrete fire episodes. The peaks data were smoothed to produce a summary of fire-episodes through time (expressed as number of episodes/1000 years). Peak magnitude represents the total accumulation of BC for all samples of a peak exceeding the threshold value, and may be related to fire size, fire intensity, and/or charcoal delivery (Whitlock et al., 2006; Higuera et al., 2007).

In a recent study, Thevenon et al. (2010) have employed the chemical/thermal oxidative method for quantification of elemental BC (i.e., the most refractory BC fractions) in oceanic and continental sediments, and the trends in the BC influx were explained to reflect regional fire activity. By contrast, the 60 hour chemical oxidation in
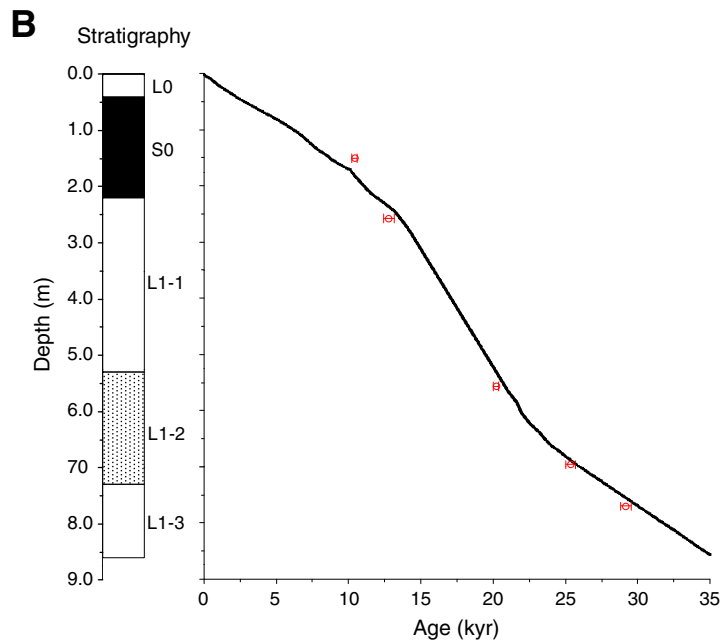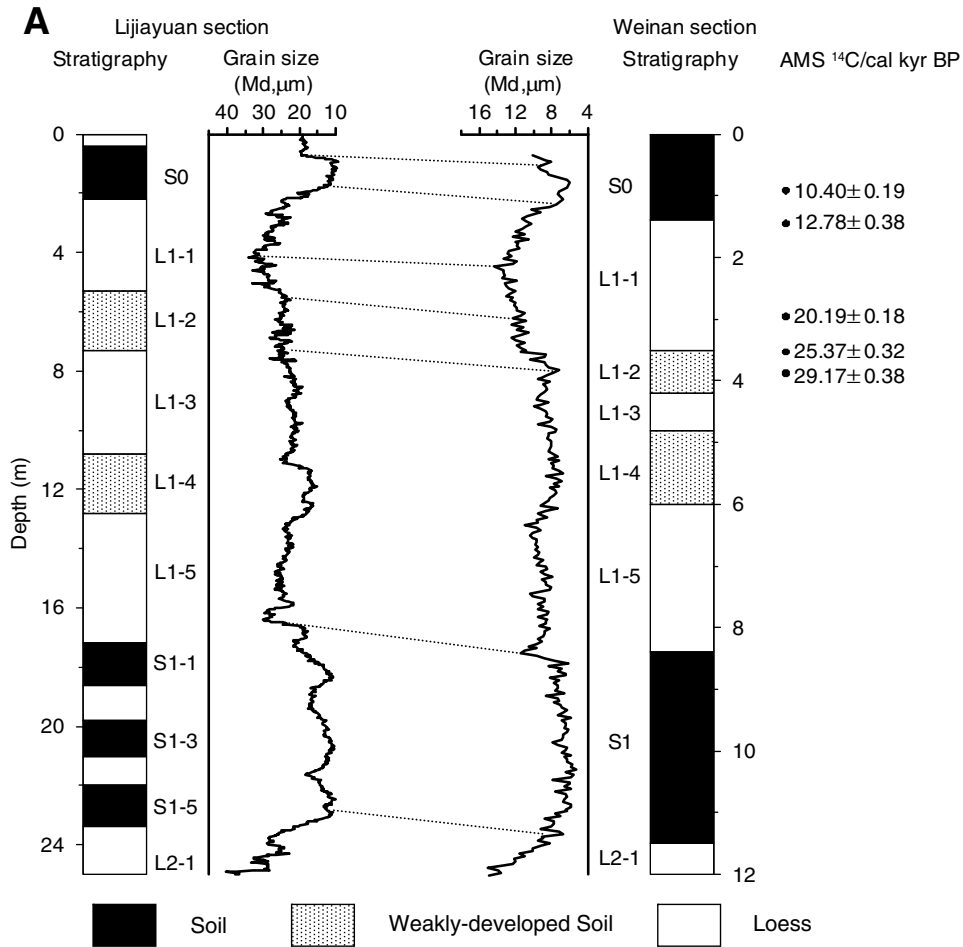
Fig. 2. Age model of the Lijiayuan loess record obtained using orbital tuning method. (A) The assumed match of the grain size profiles in depth between the Lijiayuan and Weinan sections. Dotted lines indicate the location of the 'control points' used to tie the two records. (B) Age–depth profile for the Lijiayuan loess record over the past 35 kyr. Red open circles indicate the radiocarbon dates of organic materials from Weinan loess record (Liu et al., 1994; Table 1).

our method can be considered a relatively 'soft' treatment, which cannot degrade the partly charred biomass (i.e., a short paleotracer to biomass burning). BC abundance in this study was obtained using high-temperature combustion of all pyrogenic carbonaceous particles resistant to the chemical oxidation. Therefore, it represents a continuum of combustion products, ranging from slightly charred biomass to highly condensed refractory soot, and thereby originates from both local and regional biomass burning. The sizes of those BC particles vary from several millimeters to submicron (Masiello, 2004). Some experimental fire studies have shown that a fire event will input more BC particles into its surrounding area than into a distant region (Clark et al., 1998; Lynch et al., 2004b). For example, charcoal accumulation declined sharply outside the fire, with only 1% of the measured particles transported beyond 20 m from the burn edge (Lynch et al., 2004b). In this case, the positive peaks extracted from our BCMSR record should represent local fire occurrences, whereas the background composition of BCMSR record indicates changes in regional fire incidence and biomass. Since there is only a sampling resolution of ~50–150 years, it could be hypothesized that peaks in our BC record may reflect centuries of high fire activity. This is different from the charcoal records from some high-resolution lake sediments where the positive peaks represent individual fire events.

5. Results

5.1. The median grain size, BC abundance and BCMSR records

The median grain size, BC abundance and BCMSR records for the Lijiayuan section since 27.5 kyr BP are shown in Fig. 3. The median grain size ranges from 9.3 to 34.2 μm, displaying a threefold variation in amplitude. The key feature for the grain size curve is that the millennial scale oscillations are superimposed on a trend towards a gradual increase and decrease in median grain size. By contrast, the BC abundance and BCMSR range from 0.056 to 0.779% and 0.014 to 0.484 mg C/cm^2/year, showing values that vary over 13 and 30-fold of magnitude, respectively. It is clear that the BC abundance and BCMSR curves resemble each other throughout the record. Before 22.3 kyr BP, the grain size, BC abundance and BCMSR values are low with frequent but small peaks that rise above background levels. Between 22.3 and 10 kyr BP, all of them increase dramatically. The grain size stays at high levels throughout the period and varies frequently with relatively small amplitude. By contrast, both BC abundance and BCMSR show large variation with a series of high values occurring at 20.4, 18.8, 17.6, 14.1 and 10.4 kyr BP. Moreover, these high values of BC abundance and BCMSR correspond with changes in grain size (Fig. 3). After 10 kyr BP, all of BC abundance, BCMSR and grain size values display a substantial drop to a relatively low level, and show less frequent variations than during other periods. Both BC abundance and BCMSR values vary with small magnitude respectively around 0.20% and 0.058 mg C/cm^2/year throughout the Holocene, while grain size continues to decline to 9.3 μm until 5.7 kyr BP and then increase to 19.6 μm until present.

The trends in the BCMSR variations look quite similar to trends in the BC abundances, implying that the sedimentation rates are not driving the observed trends in BCMSR when we convert the BC abundances into BCMSR data by multiplying the sedimentation rates. Therefore, the BCMSR data should represent a true reflection of varying fire occurrence.

5.2. Selection of window width and threshold ratios for Charster analysis of the BCMSR record

To help decide the appropriate width of the temporal window used to calculate the locally-weighted mean (and hence the smoothness of the background component), different window widths were examined by visually comparing the resulting background component with the BCMSR time series. Window widths <300 years mimicked the peaks

component, while window widths >900 years generalized the background component and obscured what are probably meaningful indications of regional fires during the Younger Dryas Chronozone (between approximately 12.9 and 11.5 kyr BP). For example, there are two short intervals with relatively high BCMSR (see YD-1 and YD-2 in Fig. 4) during the Younger Dryas Chronozone, corresponding to the two cold, dry phases reconstructed from pollen and δ^{13}C records on the northern Chinese Loess Plateau (Zhou et al., 1996, 2001). If we apply window widths of >900 years to the BCMSR time series, YD-2 phase would be missed in the background BCMSR. Window widths between 300 and 900 years showed similar variations in the resulting background component, and an intermediate window width of 600 years was selected as optimal (Fig. 4). At the same time, a range of threshold-ratio values from 1.00 to 1.20 were evaluated to determine an appropriate value for identifying peaks with a 600-year background window (Fig. 5). The examination mainly focuses on the similarities and reliability of the identified peak components using various threshold ratios since there are neither independent known fire events in historical documents nor any information on occurrences of fire in the vegetation type at the study location. Results show that all the threshold ratios between 1.00 and 1.12 recognize a similar occurrence of peaks though time (Fig. 5). By contrast, a threshold-ratio value of 1.20 produced a long fire-free interval (ca. 1700 years), uncharacteristic of the expected modern fire regime, especially since human activity intensified in the region during the past 2 kyr (see arrow in Fig. 5). We selected a threshold-ratio of 1.12 which, although obscuring some small peaks that may reflect local fires, produced peaks that reliably represent fire occurrences at the study location. As aforementioned, the peaks in our BC record may reflect centuries of high fire activity not individual fire events. Therefore, the inferred fire frequency should be called apparent fire frequency, which is a reconstruction of the general trend for the fire regime through time for the Lijiayuan area.

5.3. Changes in background BCMSR, apparent fire frequency and peak magnitude

Changes in background BCMSR are shown in Fig. 6, in comparison with median grain size at Lijiayuan, stalagmite δ^{18}O in central China and GISP2 δ^{18}O records. The eye-catching feature is that the background BCMSR is highly variable for the last glacial period and parallels the Dansgaard–Oeschger (D–O) climatic variability as detected in the grain size record with high values during the Younger Dryas (YD), Older Dryas (OrD), Heinrich events (HE1 and HE2) and Greenland stadials (GS, marked by number GS-1b and GS-1c) and low values during Greenland interstadials (GI, marked by number GI-1 and GI-2). During the YD Chronozone, the background BCMSR shows three phases of variation: a phase of relatively low background BCMSR bracketed by two phases of high background BCMSR, in accordance with the changes in grain size in the same section. During the Bølling–Allerød period, a pronounced increase of the background BCMSR occurred at the middle stage, corresponding with peaks of grain size. It is worth mentioning that a pronounced increase of background BCMSR occurs at the beginning of Holocene (e.g., at about 10.4 kyr), which is not documented in the median grain size or in the stalagmite and GISP2 δ^{18}O records.

The inferred apparent fire episode frequency and peak magnitude are displayed in Fig. 7. Fire activity at Lijiayuan since 27.5 kyr BP fluctuated between 1 and 6 fire episodes/1000 years and peak magnitude between 0.000044 and 0.049 mg C/cm^2/year peak^{-1}. Visual inspection of the fire episode frequency and peak magnitudes suggests that it can be divided into five distinct periods: a pre-Last Glacial Maximum (LGM) interval featuring an intermediate fire episode frequency (3–4 episodes/1000 years) and peak magnitude (0.000044–0.019 mg C/cm^2/year peak^{-1}) (27.5 to 22.3 kyr BP; zone 5), a LGM interval containing intermediate to relatively high fire episode frequency (2–6 episodes/1000 years) and peak magnitude
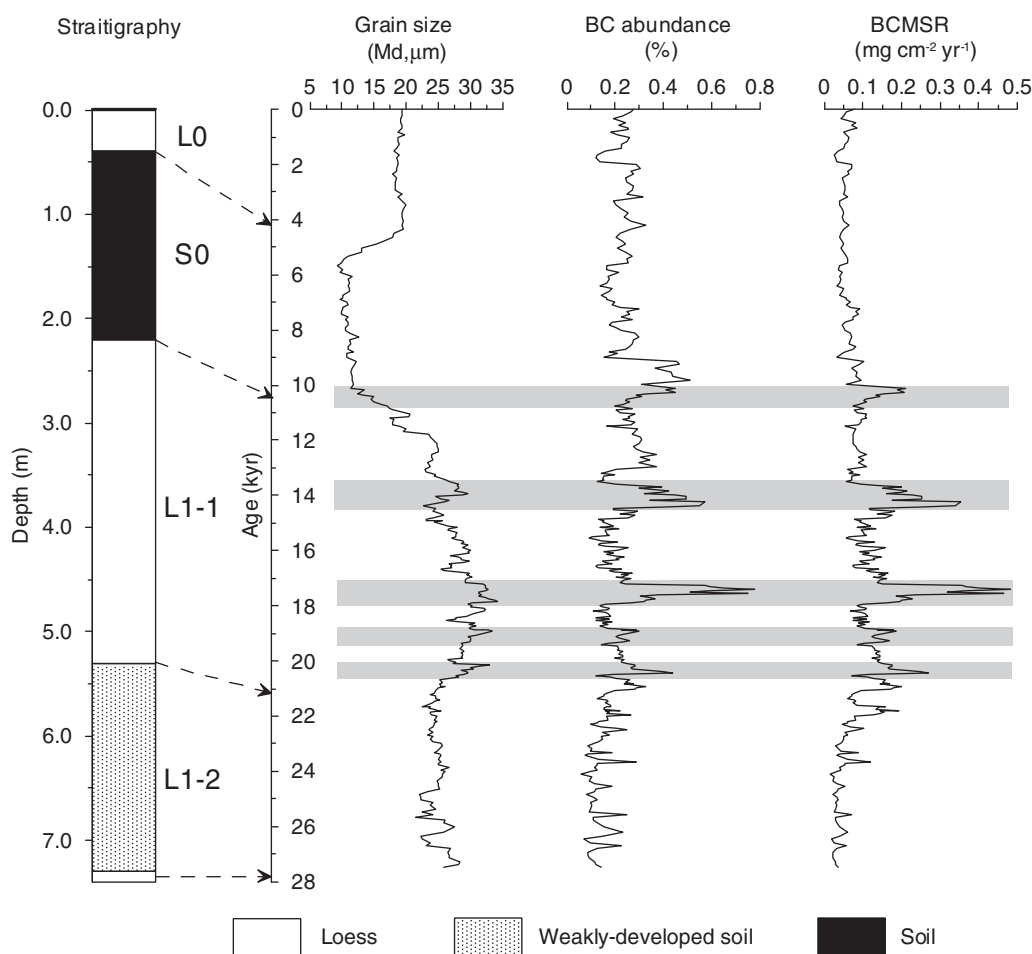
Fig. 3. BC abundance, BCMSR and grain size records plotted against age in Lijiayuan section, and correlated with the subdivision of stratigraphy, i.e., sediment type. The shaded zones indicate the correlation for high values of the three proxy indicators.

(0.00023–0.049 mg C/cm^2/year peak^{-1}) (22.3 to 14.6 kyr BP; zone 4), a last glacial–interglacial transition interval that had an intermediate to relatively low fire episode frequency (reducing from 4 to 1 episodes/1000 years) and a gradually decreasing peak magnitude (from 0.022 to 0.00074 mg C/cm^2/year peak^{-1}) (14.6 to 11.0 kyr BP; zone 3), an early-to-middle Holocene interval characterized by generally a low fire episode frequency (1–3 episodes/1000 years) and low magnitude (0.0000062–0.023 mg C/cm^2/year peak^{-1}) except for the peaks that occurred around 10.4 kyr BP (11.0 to 4.0 kyr BP; zone 2), and a late Holocene interval featuring an intermediate fire episode frequency (1–4 episodes/1000 years) and peak magnitude (0.00013–0.036 mg C/cm^2/year peak^{-1}) (4.0 kyr BP to present; zone 1) (Fig. 7).

### 5.4. Variations in carbon isotope composition of black carbon

The variations in BC carbon isotope composition compared with the subdivision of vegetation zones are displayed in Fig. 7. The δ^{13}C values of BC range from −21.83 to −24.64‰, with an average of −23.36‰ (Fig. 7). The δ^{13}C of BC between 27.5 and 22.3 kyr BP shows more positive values with relatively large variations (−22.80 ± 0.45‰), corresponding to the fluctuations of arboreal and herb pollen percentages in the region (Li et al., 2006; Tang et al., 2007). The more positive δ^{13}C values of BC occurred at about 26–24 kyr BP, which coincides with the vegetation changes from forest to steppe between 26 and 25 kyr BP in the region (Li et al., 2006). During the LGM (22.3 to 14.6 kyr BP), the δ^{13}C of BC was relatively low (e.g., −23.21 ± 0.33‰) in the early stage (22.3 to 17.6 kyr BP)

and then increased to relatively high values (−22.87 ± 0.37‰) until 14.6 kyr BP. The gradual increase of δ^{13}C values of BC during this period corresponds to an increase in upland herb percentages in the region at 18–14.6 kyr BP (Li et al., 2006). The δ^{13}C of BC decreased from 14.6 to 4.0 kyr BP, with the most negative value of −24.64‰ at 4.0 kyr BP, along with a stepwise increase of arboreal pollen from steppe via forest-steppe to coniferous-broadleaved forest (see Table 1). After that time, the δ^{13}C of BC dramatically increased to −23.20‰ until 1.6 kyr BP and then declined to the present-day value of −24.30‰. Meanwhile, a steppe dominated landscape developed in the region from 4.0 to 1.0 kyr BP (Table 1; also see Sun et al., 2010).

6. Discussion

6.1. The response of regional fire activity to abrupt climate changes on the Chinese Loess Plateau

In recent studies, background charcoal trends have been interpreted as a record of regional fire activity (Clark and Royall, 1995a; Clark and Patterson, 1997; Whitlock and Bartlein, 2004; Marlon et al., 2006; Higuera et al., 2007). Meanwhile, background charcoal has also been considered to represent the relative amount of biomass burned (Marlon et al., 2009). Since the vegetation in our study area has not significantly changed since 27.5 kyr BP except for the mid-Holocene (7.6–4.0 kyr BP) when coniferous-broadleaved forest developed (Table 1 and Fig. 7), the relative amount of biomass burned should not vary to a large extent. Therefore, the background BCMSR in our record must reflect changes in regional biomass burning.
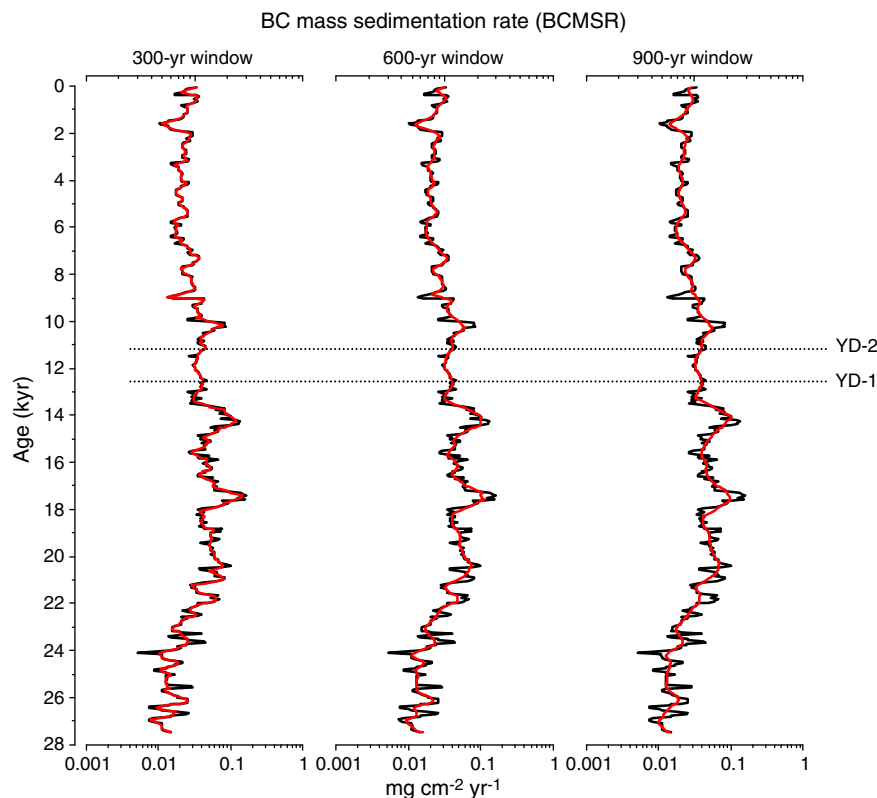
Fig. 4. Comparison of window widths of 300, 600, and 900 years in defining background levels of log-transformed BCMSR. Values interpolated to a constant time step. The red lines indicate background BCMSR. The horizontal dotted lines mark two intervals of high fire activity corresponding to two dry phases (YD-1 and YD-2) in the Younger Dryas Chronozone. The intermediate width of 600 years was used for the fire-history reconstruction.

The grain size of the loess on the Loess Plateau can be affected by several factors, including source-to-sink distance, transporting wind intensity and post-depositional weathering. Previous studies have emphasized the effect of wind intensity on loess grain size (An et al., 1991; Xiao et al., 1995; Lu and An, 1998; Sun et al., 2006). The winter monsoon winds may have been stronger during glacial periods than during interglacial periods and are thought to be responsible for the coarsening of the glacial loess. However, more recent studies suggest that the dominant factor controlling grain size is source-to-sink distance, i.e., a southward advance of the deserts leads to an increase in loess grain size and vice versa (Ding et al., 1999; Yang and Ding, 2004; Ding et al., 2005; Yang and Ding, 2008). The relatively proximity of the desert is tightly linked to wet–dry cycles (Sun et al., 1998; Yang and Ding, 2008). For example, cold dry climates allow deserts to expand closer to the site and therefore larger grain sizes fall out first, while during wet climates deserts are further away and only smaller grain sizes make it to the site. Therefore, the changes in our grain size record reflect the oscillation of dry and wet conditions.

In this study, a close correlation between changes in background BCMSR and grain size on millennial time scales can be observed during last glacial period. For example, the high values in both the background BCMSR and grain size occurred during the Younger Dryas (YD), Older Dryas (OrD), Hienrich events (HE1 and HE2) and Greenland stadials (GS-1b and GS-1c), whereas low values are recorded during Greenland interstadials (Fig. 6). The high values in grain size during the stadials suggest dry conditions usually accompanied by cold climatic events on the Chinese Loess Plateau. Therefore, the high background BCMSR occurring during stadials indicates a rapid response of regional fire activity on the Chinese Loess Plateau to abrupt climate changes, i.e., wet–dry oscillations on millennial time scales.

During the YD Chronozone, the background BCMSR shows three phases: a phase of relatively low background BCMSR bracketed by two phases of high background BCMSR (Fig. 6). This indicates that a strong fire regime existed during the early and late stages of the YD Chronozone while a weak fire regime occurred in the middle stage. An increase in fire regime is associated with dry conditions as indicated by larger grain size values during the early and late stages, and low fire regime with wet conditions during the middle stage. Pollen and δ^{13}C studies in northern Chinese Loess Plateau sections (Zhou et al., 1996, 2001) have shown that the climate of the YD Chronozone experienced an oscillation from cold-dry to cool-humid to cold-dry conditions, with elevated pollen values from broad-leaved deciduous trees, *Betula*, and aquatic plants in the middle phase. Thus both the climate and ecology supports the changes in fire regimes during the YD Chronozone in this study.

At the same time, during the Bølling–Allerød (B/A) warm period, the pronounced increase in the background BCMSR reflects a higher fire regime occurring during the middle stage associated with the dry climates as indicated by the grain size record. This high fire regime stage corresponds to the Older Dryas (OrD) cold event as recognized by some recent paleoclimatic studies in Europe (Von Grafenstein et al., 1999; Brauer et al., 2000; Zolitzschka et al., 2000). On the northern Chinese Loess Plateau, Zhou et al. (1999) have observed a cold and dry phase in the middle part of B/A interstadial via a δ^{13}C proxy curve. This further indicates the existence of the OrD cold event on the Chinese Loess Plateau. The variability of background BCMSR within both the YD Chronozone and B/A interstadial may suggest a rapid response of regional fire activity even to century-scale fluctuations in East Asian monsoon paleoclimatic events.

Heinrich events that are indicated by beds of ice-rafted detritus in North Atlantic sediments have been recognized as horizons with coarser particles on the Chinese Loess Plateau in many recent studies (Porter and An, 1995; Ren et al., 1996; Chen et al., 1997; Ding et al.,
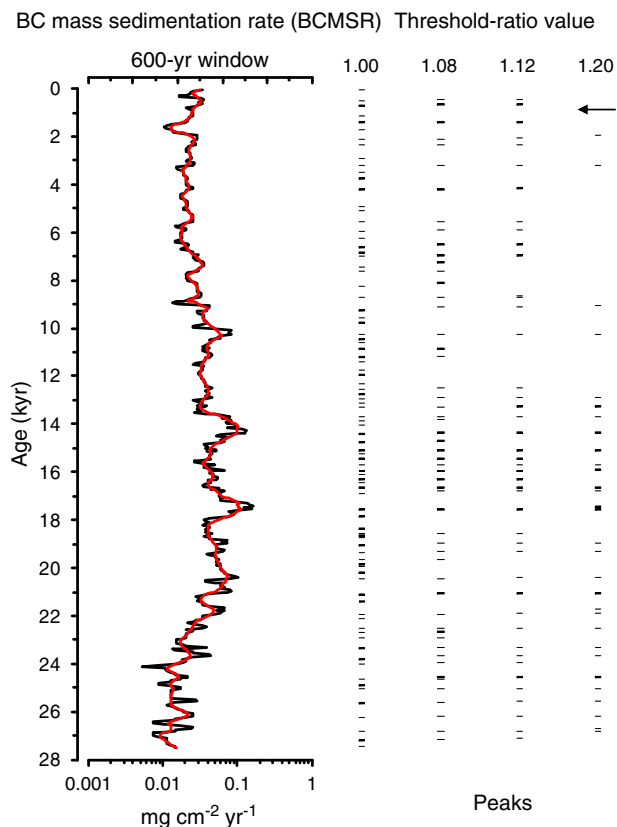
Fig. 5. Comparison of threshold-ratio values of 1.00, 1.08, 1.12, and 1.20 in the detection of peaks in log-transformed BCMSR using a background window width of 600 years. The red line indicates background BCMSR. Peaks (−) indicate a fire event. The arrow indicates the ca. 1700-year fire-free period discussed in the text. The threshold-ratio value of 1.12 was selected for the fire-history reconstruction.

1998a, 1998b). The general notion is that during the HE periods, the winter monsoon over East Asia increased and the summer monsoon decreased, leading to the expansion of deserts in central Asia, and thus recorded in the loess horizons with coarser particles. Our background BCMSR record in Lijiayuan section shows that high regional fire activity occurred during the HE periods contemporaneous with the dry climates and the sudden decreases in woody plants as shown in pollen assemblages in the region (Li et al., 2006). Therefore, the expansion of steppe under cold and dry conditions during the HE periods promoted the propagation of fire over the landscape.

The rapid response of regional fire activity on the Chinese Loess Plateau to abrupt climate changes may be explained by three physical processes. (1) Relatively dry climates persisting during the YD, OrD, HE and GS periods favoring the expansion of grassland and allowing more continuous fuel buildup that promoted fire. At the same time, the dry climate could also lengthen the fire season by reducing the number of rainy days in summer, thus increasing the probability of fire occurrences. (2) A strengthened dry winter monsoon wind during these cold periods facilitating an increase in fuel desiccation and promoting the propagation of fires over the landscape once they were ignited. (3) An increased frequency of dry lightning storms occurring due to an atmospheric reorganization during the periods of abrupt climate changes, which would favor fire ignitions under the circumstances of increased availability of dry biomass. By contrast, wet climates occurring in GI periods resulted in increases in woody vegetation and less continuous wet fuels in the summer months, leading to low fire regimes.

A similar pattern of fire occurrence was also observed in BC or charcoal records from the southern part of the Chinese Loess plateau

(Yang et al., 2001) and from sites in southern China (Jia et al., 2000; Sun et al., 2000). The coherency suggests that the millennial scale climate variability created similar widespread conditions influencing fire weather, fuel buildup and fire severity (biomass consumed) across the regions and, therefore, climate is the dominant driving factor for fire regimes on the Chinese Loess Plateau and even in southern China. Climate as the dominant driving factor also exists in the northwestern USA at the regional scale (e.g., Whitlock et al., 2008). By contrast, a different fire regime has been observed in southwestern Iberia (Daniau et al., 2007) and western France (Daniau et al., 2009), where low fire regimes associated with open vegetation during Greenland stadials including Heinrich events contrast with high fire regimes associated with open forest during Greenland interstadials. This reveals regional differences in climate conditions determining vegetation type, amount of fuel and fire weather.

To examine the periodicity of the regional fire activities, spectral analysis was conducted on the background BCMSR time series. Power spectra of the analyzed time series show statistically significant periodicities at the 90% confidence level at periods of 3440, 1620 and 1040 years (Fig. 8). The 1620 and 1040 years periodicities for regional fire activities are very close to the 1.6 and 1.2 kyr cycles of the East Asian monsoon as registered in the speleothem records from central China (see Wang et al., 2008). This further testifies to the first order control of millennial-scale monsoonal wet–dry cycles on regional fire activity on the Loess Plateau. This type of fire regime is also noticed in some modern fire studies. For example, widespread fires occur in dry/cool years, but wet/warm years are associated with little fire activity in the grasslands of the Chinese Loess Plateau (Li, 2006; Zhang et al., 2007). In addition, the observed periodicities of regional fires on the Chinese Loess Plateau are also comparable to the 1470 ± 500 years cyclicity of North Atlantic ice-rafted debris (Bond et al., 1997) and the 1667 and 1190 years of Greenland interstadial cycles (Clemens, 2005), showing a strong linkage of wet–dry oscillations in monsoonal climate on the Chinese Loess Plateau to global climate. The paleoclimates between the high latitude/polar areas and the East Asian monsoon areas may be connected through cold air mass activity via the westerlies and the related atmospheric pressure system (Zhou et al., 1996, 1999; An, 2000).

6.2. Local fire activity in the Lijiayuan area and its linkage to changes in climate and vegetation

The variations in fire episode frequency and fire size respectively inferred from the positive peaks and the peak magnitudes of the BCMSR record at Lijiayuan reflect a shift in the local fire regime over time. In addition, $\delta^{13}C$ values of BC can provide information on the type of vegetation consumed (e.g., Bird and Grocke, 1997; Jia et al., 2003). Here we discuss the local fire regimes at different time periods and potential linkage to changes in climate and vegetation in the Lijiayuan area.

It is well known that C4 plants ($\delta^{13}C_{mean} = -13‰$), mainly grasses and some bushes, are isotopically different from C3 plants ($\delta^{13}C_{mean} = -27‰$), which are composed mainly of xylophyta (Farquhar et al., 1989). Moreover, some studies have shown that the $\delta^{13}C$ range of the combustion aerosol is from −20 to −24‰ for savannah grasses and from −25 to −30‰ for trees (Cachier et al., 1989). If we take the mean $\delta^{13}C$ values of −22‰ and −27.5‰ as the end members of carbon isotope composition for BC produced from grasses and trees respectively, then the mean $\delta^{13}C$ value of BC of −23.36‰ (range: −21.83 to −24.64‰) in our record (Fig. 7) may indicate that the burnt vegetation was mostly grasses. This is consistent with the widespread grassland with some woody species oscillation between the glacial and interglacial periods as shown by pollen studies on the Loess Plateau (Sun et al., 1997; Li et al., 2003; Jiang and Ding, 2005).

During the pre-LGM period (27.5 to 22.3 kyr BP), fire occurrence was characterized by an intermediate fire frequency (e.g., 3–4
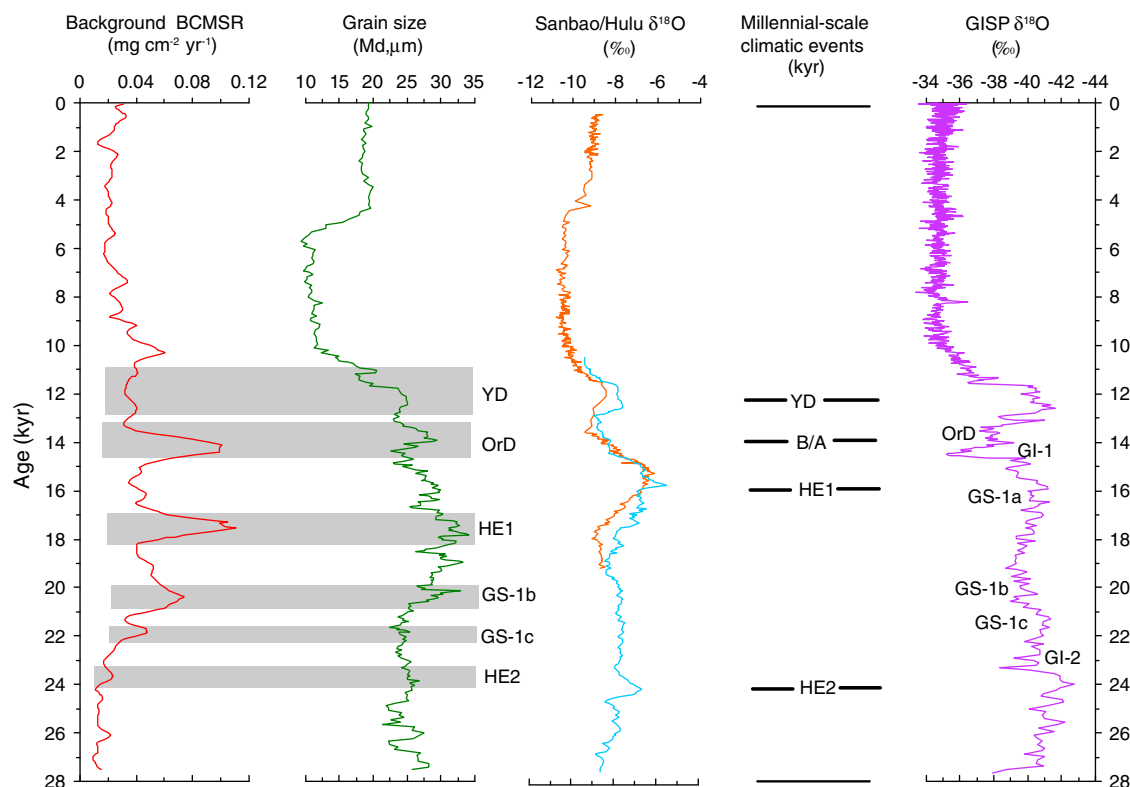
Fig. 6. Comparison of the background BCMSR with grain size at Lijiayuan, Sanbo/Hulu stalagmite $\delta^{18}O$ values in central China and GISP2 Ice Core $\delta^{18}O$ record in Greenland. For comparison, the Hulu $\delta^{18}O$ record (orange) is plotted 1.6‰ more negative to account for the higher Hulu values than Sanbao cave (blue) (see Wang et al., 2008). Note that high background BCMSR values occurred during the Younger Dryas (YD), Older Dryas (OrD), Heinrich events (HE1 and HE2) and Greenland stadials (GS-1b and GS-1c).

episodes/1000 years) and intermediate fire size. At this time, $\delta^{13}C$ values of BC show more positive values with relatively large variations (-22.80 ± 0.45‰), indicating the vegetation had a varied composition but was mainly composed of grasses. Similarly, pollen analysis in the region suggests fluctuations in woody (*Pinus* and *Picea*)/grass (Compositae, *Artemisa*, Gramineae and Chenopodiaceae) species, indicating a generally temperate/humid climate with some intervening warm/dry phases (Table 1; Tang et al., 2007). This is consistent with the relatively low median grain size values with small frequent variations before 22.3 kyr BP (Fig. 6). The changes in wet–dry conditions and vegetation are conducive to two different fire regimes: (1) during the temperate/humid climate periods, the succession of some woody species allows buildup of less continuous wet fuels, resulting in less frequent and small fires; and (2) during the intervening dry periods, the succession of grass species favors accumulation of fine fuels and an increase in fuel continuity, which is necessary to spread fires, promoting more frequent and large fires. Therefore, the fire regime with intermediate fire frequency and fire size occurred during this period.

During the last glacial maximum (LGM) period (22.3 to 14.6 kyr BP), changes in fire episode frequency and fire size can be divided into two stages. During early stage (22.3 to 17.3 kyr BP), fire episode frequency was low to intermediate (e.g., 2–3 episodes/1000 years) but with intermediate to relatively high peak magnitudes. The $\delta^{13}C$ values of BC (-23.15 ± 0.33‰) were slightly more negative and show a trend towards slightly more negative values, indicating an increasing portion of grassy fuels in the burnt vegetation. This is in accordance with the gradually intensified cold and dry climate as evidenced by increased grain sizes (Fig. 6). Pollen assemblages suggest that open steppe developed in the region during this period (Table 1). At this time, the higher peak magnitudes suggest the fires may have been larger and/or more intense in the Lijiayuan area and produced more BC. The longer duration of BCMSR peaks at 17.5,

18.9, 19.3, 21.0 and 21.8 kyr BP may reflect some intervals with centuries of high fire activity (Fig. 7), corresponding to regional fire occurrences during Hienrich events (HE1) and Greenland stadials (GS-1b and GS-1c) (Fig. 6). During the late stage (17.3 to 14.6 kyr BP), fire episode frequency was high (4–6 episodes/1000 years) with a maximum of 6 episodes/1000 years at 16.1 kyr BP and the peak magnitudes were generally low to intermediate, reflecting smaller and/or less intense fires occurring more frequently. This stage corresponds to the period of more positive $\delta^{13}C$ values of BC (-22.95 ± 0.26‰), suggesting that the portion of grassy fuels continue to increase in burnt vegetation. Meanwhile, pollen assemblages in the region indicate desert steppe to grassy steppe with low vegetation cover during this stage (Table 1; Tang et al., 2007). The low fuel load may account for the smaller and/or less intense fires during the late stage whereas the relatively high fuel load probably promoted larger and/or more intense fires during the early stage. In short, fire occurrence during LGM period was characterized by combined infrequent large fires (or high fire activity intervals) and frequent small fires, showing the rapid response of local fires in the Lijiayuan area to millennial and/or centurial variability of the monsoonal climate.

During the last glacial–interglacial transition period (14.6 to 11.0 kyr BP), fire incidence showed an abrupt decline to a minimum of one episode/1000 years and peak magnitudes also displayed a drop from intermediate to a very low level. At this time, an overall decrease occurred in $\delta^{13}C$ values of BC from -22.69‰ to -23.75‰, consistent with the establishment of xeric woodland (e.g., mainly conifers) due to the initiation of a warm/humid climate as indicated by pollen assemblages in the region (Tang et al., 2007). A stepwise decrease in the grain size record during this transition period (Fig. 6) indicates a gradually intensified summer monsoon which brought more precipitation. Therefore, a higher moisture level of the woody coarse fuels may have greatly reduced the probability of fires even in the presence of ignition sources and less continuous
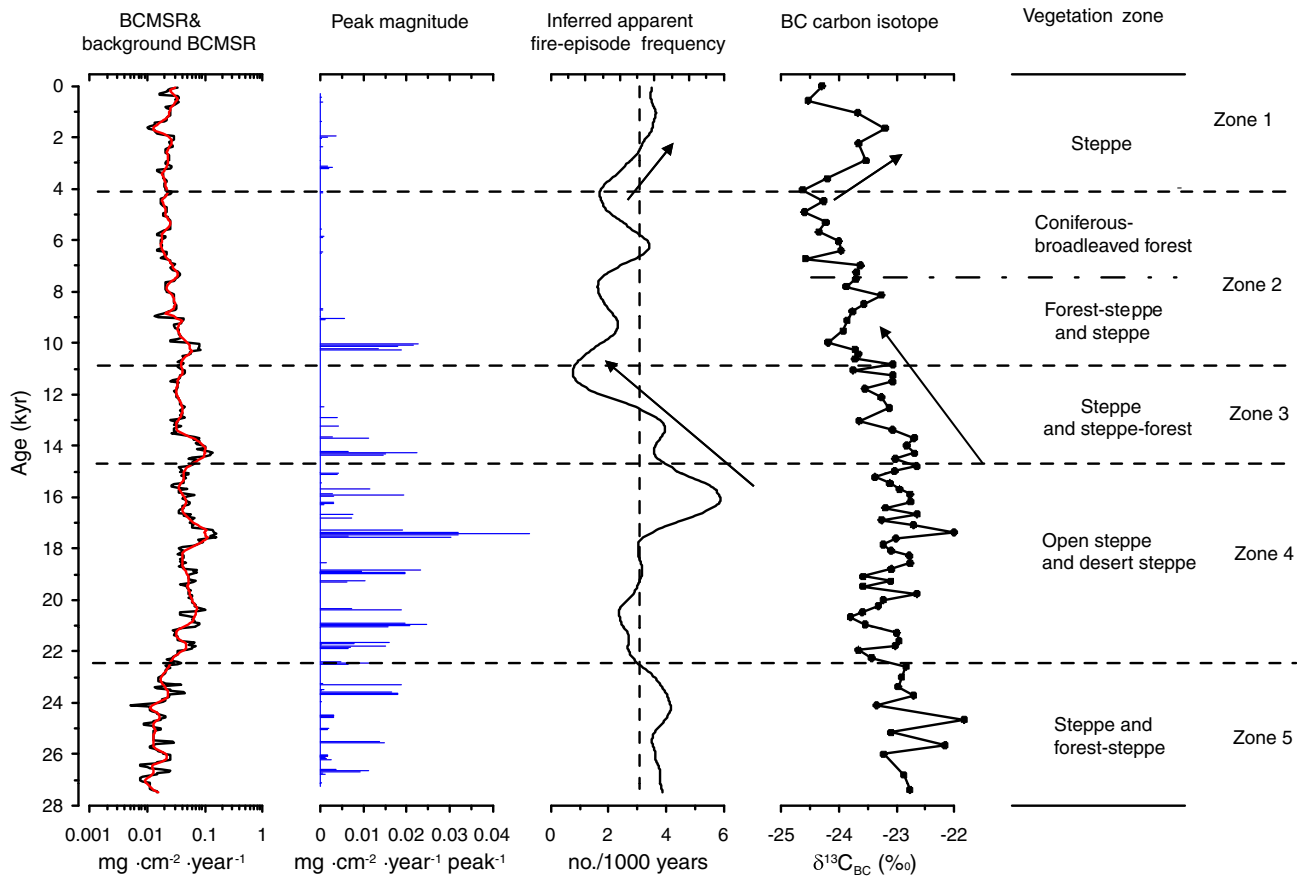
Fig. 7. Log-transformed BCMSR, background level, peak magnitudes, and inferred fire episode frequency for Lijiayuan section, using a background window width of 600 years and a threshold-ratio value of 1.12. The red line indicates background BCMSR. Horizontal lines denote boundaries between zone 5 (pre-LGM, ca. 27.5 to 22.3 kyr BP), zone 4 (LGM, ca. 22.3 to 14.6 kyr BP), zone 3 (Late glacial–interglacial transition, ca. 14.6 to 11.0 kyr BP), zone 2 (early to middle Holocene, ca. 11.0 to 4.0 kyr BP), and zone 1 (late Holocene, ca. 4.0 kyr BP to present).

wet fuels would prevent fire spreading even if ignition occurred, leading to an abrupt decline in fire episode frequency and fire size.

The last glacial–interglacial transition experienced the last major natural global warming in association with an increase in Greenhouse gases, thus providing an analog to future climate changes. Recently, most modeling studies have projected increased monsoon precipitation in East Asia under future CO_2-induced global warming (e.g., Kimoto, 2005; Kripalani et al., 2007; Sun and Ding, 2010). In this scenario, we predict that future global warming would largely reduce the fire incidence in northwestern China. This is quite different from what is projected in North America where more frequent fires have been assumed to occur under future conditions (e.g., International Panel on Climate Change, 2007; U.S. Climate Change Science Program, 2008). The difference in the fire regimes between Northwestern China and North America may be related to the different fire weather over the two continents. On the Chinese Loess Plateau, most rainfall occurs in summer when temperature is high (Wang et al., 2005), keeping fire danger low during this season. By contrast, both high temperatures and low rainfall occur in summer in western United States, increasing wildfire activity for most of the summer (Westerling et al., 2006). This suggests that different fire regimes over continents should be considered in current assessments of the effects of climate changes on wildfires and resultant carbon emissions at the global scale.

During the early-to-middle Holocene (11.0 to 4.0 kyr BP), fire occurrence was generally low but showed a large variation between 1 and 3 episodes/1000 years. For example, fire episode frequency was 1 to 2 episodes/1000 years during the early Holocene (11.0 to 8.0 kyr BP) and then increased to more than 3 episodes/1000 years during the middle Holocene (7.0 to 6.0 kyr BP). Accordingly, peak

magnitudes almost dropped to their lowest level except for those at about 10.4 kyr BP. The $\delta^{13}C$ values of BC continued to decline and reached the lowest value of $-24.64‰$ at 4.0 kyr BP, which is consistent with the gradual development of conifer forest and deciduous forest in the region (Table 1). The grain size during this period was at its lowest level for the record (Fig. 6), suggesting a persistently warm and humid climate. The wet climate during this period may largely have reduced the occurrence and size of biomass burning. However, the relatively high fire frequency during the period 7.0 to 6.0 kyr BP may possibly have resulted from increased human fires, as discussed below.

During the late Holocene (4.0 kyr BP to present), fire incidence gradually increased to a maximum of 4 episodes/1000 years by 1.0 kyr BP and peak magnitudes remained at a low level but showed a slight increase with respect to middle Holocene. Meanwhile, $\delta^{13}C$ of BC dramatically increased to $-23.20‰$ at 1.6 kyr BP and then declined to the present-day value of $-24.30‰$, consistent with the development of a steppe dominated landscape in the region from 4.0 to 1.0 kyr BP (Table 1; also see Sun et al., 2010). The grain size during this period increased significantly (Fig. 6), indicative of a drier climate. High fire activity was undoubtedly associated with the presence of xeric steppe vegetation and a drier climate. However, intensification of human activities during the late Holocene may also have contributed to the increase in fire frequency.

6.3. Possible influence of human activities on fires since the mid-Holocene

Despite the apparent climate control on fire activity, human colonization and social change are also important factors (Pyne and

Table 1
Vegetation, climate and pollen groups in western part of the Chinese Loess Plateau.[a]

Age (kyr BP)	Vegetation type	Climate	Pollen assemblage
4.0–1.0	Steppe	Cool and dry	Grass pollen dominates, including Compositae, *Artemisia*, Gramineae and Chenopodiaceae. *Pinus* and *Ulmus* also present.
7.6–4.0	Temperate mixed coniferous-broadleaved forest	Warm and humid	High pollen yielding. Coniferous pollen includes *Pinus*, *Picea* and *Abie*. Deciduous tree pollen includes *Betula*, *Corylus*, *Quercus* and *Ulmus*, etc. Some grass pollen is mainly from Gramineae, Compositae, Chenopodiaceae, *Typha* and Cyperaceae.
11.0–7.6	Forest-steppe and Steppe	Warm and semi-wet	Woody pollen increased, and mainly from *Pinus*, *Sabina*, Cupressaceae, *Juglans*, *Ulmus*, *Quercus*. Grass pollen is still rich, including Compositae, *Artemisia*, Gramineae and Ranunculaceae.
14.6–11.0	Steppe-forest	Warm and semi-wet	Woody pollen dominates, including mainly *Pinus* and *Picea*, with some Cupressaceae and *Ulmus*. Grass pollen decreased, and composed of Compositae, *Artemisia*, Gramineae and Chenopodiaceae.
23.0–14.6	Open steppe and desert steppe	Cold and dry	Grass pollen dominates, including Compositae, *Artemisia* and Chenopodiaceae. *Pinus*, *Picea*, Cupressaceae and *Ulmus* also present.
27.5–23.0	Steppe and Forest-steppe	Temperate and humid	Both woody and grass pollen show significant fluctuation. Woody pollen includes mainly *Pinus* and *Picea*, with some *Ulmus* and *Betula*. Grass pollen is composed of Compositae, *Artemisia*, Gramineae and Chenopodiaceae.

[a] Results are compiled from the pollen studies in Jingning, Dingxi, Qin'an and Haiyuan area (see Li et al., 2006; Tang et al., 2007; Sun et al., 2010).

Goldamer, 1990). The earliest known Neolithic culture on the western Loess Plateau is the Dadiwan Culture (7800–7350 cal. years BP), followed by the Yangshao Culture (6800–4900 cal. years BP), Majiayao Culture (5300–4300 cal. years BP) and the Qijia Culture (4300–3900 cal. years BP) (Shui, 2001). The prosperity of the Neolithic cultures on the western Loess Plateau appeared between 6300 and 4000 cal. years BP when the climate changed from wet to semi-arid, and the increased aridity was more favorable to cereal-based agriculture focused on drought-adapted crops such as millet (An et al., 2004). Since then, intensity of human disturbance by fire and cultivation increased continuously on the Chinese Loess Plateau (e.g., Huang et al., 2006).

The uppermost loess layer (L0) is ubiquitously distributed over the Loess Plateau, and was thought to have formed due to an abrupt shift from the southeastern monsoon to northwestern monsoon (Zhang and Hu, 1989). However, another possible explanation for the appearance of L0 may be the land cover change associated with the intensified cereal-based agriculture (Huang et al., 2006). The timing of the boundary between L0 and the underlying paleosol S0 in this study was around

Fig. 8. Spectral analysis results of the background BCMSR time series. Plots are bias-corrected spectrum (thin solid line) and false-alarm level. Horizontal bar indicates 6-dB bandwidth (BW) (0.145 kyr^{-1}), which determines the frequency resolution. The red-noise alternative is upper 90% χ^2 bound (smooth line) from a first-order autoregressive (AR1) process. The spectra were estimated using the program REDFIT (Schulz and Mudelsee, 2002) with OFAC = 4 and HIFAC = 1. The 1000 Monte-Carlo simulations were used for the bias-correction. The spectral window is a Welch I type.
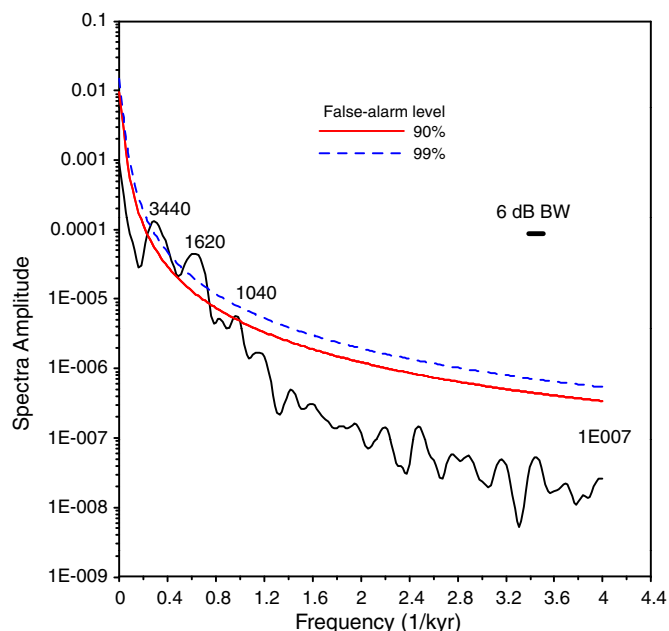
4.3 kyr BP (Fig. 3), which compares favorably with the dating of L0/S0 boundary in the adjacent areas of the Loess Plateau (Zhang and Hu, 1989; Hu, 1994). This may suggest that cereal-based agriculture has been widespread on the Chinese Loess Plateau since the late Holocene. Therefore, the increase in fire episode frequency at Lijiayuan since 4.0 kyr BP (Fig. 7) may be related to intensified land cultivation. On the southern Chinese Loess Plateau, charcoal records reveal that frequent biomass burning has occurred through the late Holocene, which is thought to be related to land reclamation for arable farming during the late Bronze Age and the early Iron Age (3100–1500 years BP) (Huang et al., 2006). The sychronical occurrence of frequent fires as recorded in different areas further supports the occurrence of widespread agriculture activity on the Chinese Loess Plateau during the late Holocene.

The high fire episode frequency during the period of wet conditions between 7.0 and 6.0 kyr BP (Fig. 7) is also likely the result of human land use when the Yangshao Culture (6800–4900 cal. years BP) developed on the western Loess Plateau (Shui, 2001). A recent pollen and charcoal study in the central part of Chinese Loess Plateau indicates increased agricultural activity and the expansion of human populations in the Guanzhong Basin between 7700 and 5500 cal. years BP (Li et al., 2009). Meanwhile, more frequent human fires inferred from large-sized charcoal peaks record also occurred on the southern Loess Plateau between 7800 and 5500 cal. years BP (Huang et al., 2006). This may suggest that the early agriculture activities during the period of the Yangshao Neolithic culture (6800–4900 cal. years BP) was well developed over the Chinese Loess Plateau due to the optimum climatic conditions of the mid-Holocene.

7. Conclusion

In this paper, we have presented the linkages of past fires to vegetation and abrupt climate changes on the Chinese Loess Plateau through comparing a BC record at Lijiayuan with associated pollen data and other paleoclimatic proxies. Moreover, the impacts of human occupation since the middle Holocene on fire activities were also discussed. The following conclusive remarks are obtained:

(1) Both BC abundance and background BCMSR have shown that high fire activities occurred contemporaneous with the Younger Dryas, Older Dryas, Heinrich events and Greenland stadials as registered in the loess grain size record, indicating a rapid response of regional fires on the Chinese Loess Plateau to abrupt climate changes. Furthermore, spectral analysis of background BCMSR showed two meaningful periodicities of 1620 and 1040 year, close to the cyclicity of the East Asian Monsoon as recorded in the central China stalagmite δ^{18}O record, indicating a tight control of millennial scale wet–dry changes in monsoonal climate on regional fires over the Loess Plateau.

(2) BC carbon isotope can detect the changes in vegetation being burnt (i.e. grasses versus trees). Isotope data show that steppe dominated the region during the LGM, then woody vegetation gradually increased during the early Holocene, and forest developed during the middle Holocene, whereas steppe has occupied the region in the late Holocene. These changes are consistent with the associated pollen data in the region.

(3) The inferred apparent fire episode frequency at Lijiayuan during the LGM was higher than that during the Holocene, manifesting the key influence of monsoonal moisture on fire occurrence. Specifically, drier conditions during the LGM on the Loess Plateau allowed for more continuous fuel buildup that promoted fire, while wet conditions resulted in increases in woody vegetation and less continuous wet fuels in the summer months.

(4) The increase in apparent fire episode frequency at Lijiayuan since 4.0 kyr BP may be to some extent related to the intensified land cultivation at that time although the dry climate would have promoted fire occurrences. Moreover, the relatively high fire episode frequency during the period of wet conditions between 7.0 and 6.0 kyr BP is also likely the result of human land use when the Yangshao Culture (6800–4900 cal. years BP) developed on the western Loess Plateau.

Acknowledgments

References

An, Z.S., 2000. The history and variability of the East Asian paleomonsoon climate. Quaternary Science Reviews 19, 171–187.

An, Z.S., Kukla, G., Porter, S.C., Xiao, J.L., 1991. Late Quaternary dust flow on the Chinese Loess Plateau. Catena 18, 125–132.

An, C.B., Feng, Z.D., Tang, L.Y., 2004. Environmental change and cultural response between 8000 and 4000 cal. yr BP in the western Loess Plateau, northwest China. Journal of Quaternary Science 19, 529–535.

Bird, M.I., Grocke, D.R., 1997. Determination of the abundance and carbon isotope composition of elemental carbon in sediments. Geochimica et Cosmochimica Acta 61, 3413–3423.

Bond, G., Showers, W., Cheseby, M., Lotti, R., Almasi, P., deMenocal, P., Priore, P., Cullen, H., Hajdas, I., Bonani, G., 1997. A pervasive millennial-scale cycle in North Atlantic Holocene and Glacial climates. Science 278, 1257–1266.

Brauer, A., Günter, C., Johnsen, S.J., Negendank, J.F.W., 2000. Land-ice teleconnections of cold climatic periods during the last Glacial/Interglacial transition. Climate Dynamics 16, 229–239.

Cachier, H., Bremond, M.P., Buat-Menard, P., 1989. Carbonaceous aerosols from different tropical biomass burning sources. Nature 340, 371–373.

Cao, Y.F., Huang, C.C., Han, J.Q., Li, U.G., Zhang, S.S., 2007. Changes of fire environment recorded by charcoal hided in Holocene profiles in the Eastern and Western Loess Plateau. Geography and Geo-Information Science 23, 92–96 (in Chinese with English abstract).

Carcaillet, C., Almquist, H., Asnong, H., Bradshaw, R.H.W., Carrion, J.S., Gaillard, M.-J., Gajewski, K., Haas, J.N., Haberle, S.G., Hadorn, P., Muller, S.D., Richard, P.J.H., Richoz, I., Rosch, M., Sanchez Goni, M.F., von Stedingk, H., Stevenson, A.C., Talon, B., Tardy, C., Tinner, W., Tryterud, E., Wick, L., Willis, K.J., 2002. Holocene biomass burning and global dynamics of the carbon cycle. Chemosphere 49, 845–863.

Chen, C.Y., 1987. A preliminary study of climate and vegetation types in loess plateau, Gansu province. Journal of Natural Resources 2, 347–358 (in Chinese with English abstract).

Chen, F.H., Bloemendal, J., Wang, J.M., Li, J.J., Oldfield, F., 1997. High-resolution multi-proxy climate records from Chinese loess: evidence for rapid climatic changes over the last 75 kyr. Palaeogeography, Palaeoclimatology, Palaeoecology 130, 323–335.

Clark, J.S., 1988. Particle motion and the theory of charcoal analysis: source area, transport, deposition, and sampling. Quaternary Research 20, 67–80.

Clark, J.S., Patterson III, W.A., 1997. Background and local charcoal in sediments: scales of fire evidence in the paleorecord. In: Clark, J.S., Cachier, H., Goldammer, J.G., Stocks, B. (Eds.), Sediment Records of Biomass Burning and Global Change. NATO ASI series. Series I, Global Environmental Change, no. 51. Springer-Verlag, Berlin, pp. 23–48.

Clark, J.S., Royall, P.D., 1995a. Particle-size evidence for source areas of charcoal accumulation in late Holocene sediments of Eastern North American Lakes. Quaternary Research 43, 80–89.

Clark, J.S., Royall, P.D., 1995b. Transformation of a northern hardwood forest by aboriginal (Iroquois) fire: charcoal evidence from Crawford Lake, Ontario, Canada. The Holocene 5, 1–9.

Clark, J.S., Royall, P.D., Chumbley, C., 1996. The role of fire during climate change in an eastern deciduous forest at Devil's Bathtub, NewYork. Ecology 77, 2148–2166.

Clark, J.S., Lynch, J., Stocks, B.J., Goldammer, J.G., 1998. Relationships between charcoal particles in air and sediments in west-central Siberia. The Holocene 8, 19–29.

Clemens, S.C., 2005. Millennial-band climate spectrum resolved and linked to centennial-scale solar cycles. Quaternary Science Reviews 24, 521–531.

Daniau, A.L., Sánchez Goñi, M.F., Beaufort, L., Laggoun-Défarge, F., Loutre, M.F., Duprat, J., 2007. Dansgaard–Oeschger climatic variability revealed by fire emissions in southwestern Iberia. Quaternary Science Reviews 26, 1369–1383.

Daniau, A.L., Sánchez Goñi, M.F., Duprat, J., 2009. Last glacial fire regime variability in western France inferred from microcharcoal preserved in core MD04-2845, Bay of Biscay. Quaternary Research 71, 385–396.

Department of geography, Shaanxi Normal University, 1987. Geography of Yulin, Shaanxi Province. Shaanxi People's Press, Xian. (351 pp.).

Ding, Z.L., Yu, Z., Rutter, N.W., Liu, T.S., 1994. Towards an orbital timescale for Chinese loess deposits. Quaternary Science Reviews 13, 39–70.

Ding, Z.L., Rutter, N.W., Liu, T.S., Ren, J.Z., Sun, J.M., Xiong, S.F., 1998a. Correlation of Dansgaard–Oeschger cycles between Greenland ice and Chinese loess. Paleoclimates 4, 281–291.

Ding, Z.L., Sun, J.M., Yu, Z.W., Liu, T.S., 1998b. Chronology of environmental events over East Asia during the past 130 ka. Chinese Science Bulletin 43, 1761–1769.

Ding, Z.L., Sun, J.M., Rutter, N.W., Rokosh, D., Liu, T.S., 1999. Changes in sand content of loess deposits along a north–south transect of the Chinese Loess Plateau and the implications for desert variations. Quaternary Research 52, 56–62.

Ding, Z.L., Yu, Z.W., Yang, S.L., Sun, J.M., Xiong, S.F., Liu, T.S., 2001. Coeval changes in grain size and sedimentation rate of eolian loess, the Chinese Loess Plateau. Geophysical Research Letters 28, 2097–2100.

Ding, Z.L., Derbyshire, E., Yang, S.L., Yu, Z.W., Xiong, S.F., Liu, T.S., 2002. Stacked 2.6-Ma grain size record from the Chinese loess based on five sections and correlation with the deep-sea ^{18}O record. Paleoceanography 17 (3), 1033. doi:10.1029/2001PA000725.

Ding, Z.L., Derbyshire, E., Yang, S.L., Sun, J.M., Liu, T.S., 2005. Stepwise expansion of desert environment across northern China in the past 3.5 Ma and implications for monsoon evolution. Earth and Planetary Science Letters 237, 45–55.

Farquhar, G.D., Ehleringer, J.R., Hubick, K.T., 1989. Carbon isotope discrimination and photosynthesis. Annual Review of Plant Physiology and Plant Molecular Biology 40, 503–537.

Gavin, D.G., unpublished data, 2006. Charster software. For detail to see http://geography.uoregon.edu/gavin/charster/Introduction.html.

Goldberg, E.D., 1985. Black Carbon in the Environment. John Wiley& Sons, New York. (198 pp.).

Higuera, P.E., Peters, M.E., Brubaker, L.B., Gavin, D.G., 2007. Understanding the origin and analysis of sediment charcoal records with a simulation model. Quaternary Science Reviews 26, 1790–1809.

Higuera, P.E., Gavin, D.G., Bartlein, P.J., Hallett, D.J., 2010. Peak detection in sediment-charcoal records: impacts of alternative data analysis methods on fire-history interpretations. International Journal of Wildland Fire 19, 996–1014.

Hu, S.X., 1994. Genesis and evolution of heilu soils in the middle and east of Gansu province. Acta Pedologica Sinica 31, 295–304 (in Chinese with English abstract).

Huang, C.C., Pang, J.L., Chen, S.E., Su, H.X., Han, J., Cao, Y.F., Zhao, W.Y., Tan, Z.H., 2006. Charcoal records of fire history in the Holocene loess–soil sequences over the southern Loess Plateau of China. Palaeogeography, Palaeoclimatology, Palaeoecology 239, 28–44.

Imbrie, J., Hays, J.D., Martinson, D.B., McIntyre, A., Mix, A.C., Morley, J.J., Pisias, N.G., Prell, W.L., Shackleton, N.J., 1984. The orbital theory of Pleistocene climate: support from a revised chronology of the marine delta ^{18}O record. In: Berger, A., Imbrie, J., Hays, J., Kukla, G., Saltzman, B. (Eds.), Milankovitch and Climate. Part I. Reidel Publishing Co., Boston, pp. 269–305.

International Panel on Climate Change, 2007. Climate change 2007: impacts, adaptation and vulnerability. In: Parry, M.L., Canziani, O.F., Palutikof, J.P., vander Linden, P.J., Hanson, C.E. (Eds.), Contribution of Working Group II to the Fourth Assessment Report of the IPCC. Cambridge University Press, Cambridge, UK. 976 pp.

Jia, G.D., Peng, P.A., Sheng, G.Y., Fu, J.M., 2000. Sedimentary records of black carbon in the sea area of the Nansha Islands since the last glaciation. Chinese Science Bulletin 45, 1594–1597.

Jia, G.D., Peng, P.A., Zhao, Q.H., Jian, Z.M., 2003. Changes in terrestrial ecosystem since 30 Ma in East Asia: Stable isotope evidence from black carbon in the South China Sea. Geology 31, 1093–1096.

Jiang, H.C., Ding, Z.L., 2005. Temporal and spatial changes of vegetation cover on the Chinese Loess Plateau through the last glacial cycle: evidence from spore-pollen records. Review of Palaeobotany and Palynology 133, 23–37.

Kimoto, M., 2005. Simulated change of the east Asian circulation under global warming scenario. Geophysical Research Letters 32, L16701. doi:10.1029/2005GL023383.

Kripalani, R.H., Oh, J.H., Chaudhari, H.S., 2007. Response of the East Asian summer monsoon to doubled atmospheric CO_2: coupled climate model simulations and projections under PCC AR4. Theoretical and Applied Climatology 87, 1–28.

Kukla, G., 1987. Loess stratigraphy in central China. Quaternary Science Reviews 6, 191–219.

Li, G.L., 2006. Monitor and control techniques of grassland fire in Gansu province. Pratacultural Science 23, 87–91 (in Chinese with English abstract).

Li, X.Q., Zhou, J., Dodson, J., 2003. The vegetation characteristic of the 'Yuan' area at Yaoxian on the Loess Plateau in China over the last 12000 years. Review of Palaeobotany and Palynology 124, 1–7.

Li, X.Q., Zhao, H.L., Yan, M.H., Wang, S.Z., 2005. Fire variations and relationship among fire and vegetation and climate during Holocene at Sanjiang Plain, Northeast China. Scientia Geographica Sinica 25, 177–182 (in Chinese with English abstract).

Li, C.H., Tang, L.Y., Feng, Z.D., Zhang, H.C., Wang, W.G., An, C.B., 2006. A high-resolution late Pleistocene record of pollen vegetation and climate change from Jingning, NW China. Science in China Series D e Earth Sciences 49, 154–162.

Li, X.Q., Shang, X., Dodson, J., Zhou, X.Y., 2009. Holocene agriculture in the Guanzhong Basin in NW China indicated by pollen and charcoal evidence. The Holocene 19, 1213–1220.

Lim, B., Cachier, H., 1996. Determination of black carbon by oxidation and thermal treatment in recent marine and lake sediments and Cretaceius–Tertiary clays. Chemical Geology 131, 143–154.

Liu, T.S., 1985. Loess and the Environment. China Ocean Press, Beijing. (251 pp.).

Liu, T.S., Ding, Z.L., 1998. Chinese loess and the paleomonsoon. Annual Review of Earth and Planetary Sciences 26, 111–145.

Liu, J.Q., Chen, T.M., Nie, G.Z., Song, C.Y., Guo, Z.T., Li, K., Gao, S.J., Qiao, Y.L., Ma, Z.B., 1994. Datings and reconstruction of the high resolution time series in the Weinan loess section of the last 150000 years. Quaternary Science 3, 193–202 (in Chinese with English abstract).

Long, C.J., Whitlock, C., Bartlein, P.J., Millspaugh, S.H., 1998. A 9000-year fire history from the Oregon Coast Range, based on a high-resolution charcoal study. Canadian Journal of Forest Research 28, 774–787.

Lu, H.Y., An, Z.S., 1998. Palaeoclimatic significance of grain size of loess–palaeosol sequence of Central China. Sci. China (ser. D) 41, 626–631.

Lynch, J.A., Hollis, J.L., Hu, F.S., 2004a. Climatic and landscape controls of the boreal forest fire regime: Holocene records from Alaska. Journal of Ecology 92, 477–489.

Lynch, J.A., Clark, J.S., Stocks, B.J., 2004b. Charcoal production, dispersal, and deposition from the Fort Providence experimental fire: interpreting fire regimes from charcoal records in boreal forests. Canadian Journal of Forest Research 34, 1642–1656.

Marlon, J.R., Bartlein, P.J., Whitlock, C., 2006. Fire–fuel–climate linkages in the north-western USA during the Holocene. The Holocene 16, 1059–1071.

Marlon, J.R., Bartlein, P.J., Walsh, M.K., Harrison, S.P., Brown, K.J., Edwards, M.E., Higuera, P.E., Power, M.J., Anderson, R.S., Briles, C., Brunelle, A., Carcaillet, C., Daniels, M., Hu, F.S., Lavoie, M., Long, C., Minckley, T., Richard, P.J.H., Scott, A.C., Shafer, D.S., Tinner, W., Umbanhowar Jr., C.E., Whitlock, C., 2009. Wildfire responses to abrupt climate change in North America. Proceedings of the National academy of Sciences of the United States of America 106, 2519–2524.

Masiello, C.A., 2004. New directions in black carbon organic geochemistry. Marine Chemistry 92, 201–213.

Millspaugh, S.H., Whitlock, C., 1995. A 750-year fire history based on lake sediment record in central Yellowstone National Park, USA. The Holocene 5, 283–292.

Ohlson, M., Tryterud, E., 2000. Interpretation of the charcoal record in forest soils: forest fires and their production and deposition of macroscopic charcoal. The Holocene 10, 519–525.

Porter, S.C., An, Z.S., 1995. Correlation between climate events in the North-Atlantic and China during the last glaciation. Nature 375, 305–308.

Power, M.J., Marlon, J., Ortiz, N., Bartlein, P.J., Harrison, S.P., Mayle, F.E., Ballouche, A., Bradshaw, R.H.W., Carcaillet, C., Cordova, C., Mooney, S., Moreno, P.I., Prentice, I.C., Thonicke, K., Tinner, W., Whitlock, C., Zhang, Y., Zhao, Y., Ali, A.A., Anderson, R.S., Beer, R., Behling, H., Briles, C., Brown, K.J., Brunelle, A., Bush, M., Camill, P., Chu, G.Q., Clark, J., Colombaroli, D., Connor, S., Daniau, A.L., Daniels, M., Dodson, J., Doughty, E., Edwards, M.E., Finsinger, W., Foster, D., Frechette, J., Gaillard, M.J., Gavin, D.G., Gobet, E., Haberle, S., Hallett, D.J., Higuera, P., Hope, G., Horn, S., Inoue, J., Kaltenrieder, P., Kennedy, L., Kong, Z.C., Larsen, C., Long, C.J., Lynch, J., Lynch, E.A., McGlone, M., Meeks, S., Mensing, S., Meyer, G., Minckley, T., Mohr, J., Nelson, D.M., New, J., Newnham, R., Noti, R., Oswald, W., Pierce, J., Richard, P.J.H., Rowe, C., Goni, M.F.S., Shuman, B.N., Takahara, H., Toney, J., Turney, C., Urrego-Sanchez, D.H., Umbanhowar, C., Vandergoes, M., Vanniere, B., Vescovi, E., Walsh, M., Wang, X., Williams, N., Wilmshurst, J., Zhang, J.H., 2008. Changes in fire regimes since the Last Glacial Maximum: an assessment based on a global synthesis and analysis of charcoal data. Climate Dynamics 30, 887–907.

Pyne, S.J., Goldamer, J.G., 1990. The culture of fire: an introduction to anthropogenic fire activity. In: Goldamer, J.G. (Ed.), Sediment Record of Biomass Burning and Global Change. Springer, Berlin, pp. 71–115.

Ren, J.Z., Ding, Z.L., Liu, D.S., Sun, J.M., Zhou, X.Q., 1996. Climatic changes on millennial time scales—evidence from a high-resolution loess record. Sci. China (ser. D) 39, 449–459.

Schmidt, M.W.I., Noack, A.G., 2000. Black carbon in soils and sediments: analysis, distribution, implications, and current challenges. Global Biogeochemical Cycles 14, 777–793.

Schulz, M., Mudelsee, M., 2002. REDFIT: estimating red-noise spectra directly from unevenly spaced paleoclimatic time series. Computational Geosciences 28, 421–426.

Shui, T., 2001. Papers on the Bronze Age Archaeology of Northwest. China Science Press, Beijing. (in Chinese).

Sun, Y., Ding, Y.H., 2010. A projection of future changes in summer precipitation and monsoon in East Asia. Sci. China (ser. D) 53, 284–300.

Sun, X.J., Song, C.Q., Wang, F.Y., Sun, M.R., 1997. Vegetation history of the Loess Plateau of China during the last 100,000 years based on pollen data. Quaternary International 37, 25–36.

Sun, J.M., Ding, Z.L., Liu, T.S., 1998. Desert distribution during the glacial maximum and climatic optimum: example of China. Episodes 21, 28–31.

Sun, X.J., Li, X., Chen, H.C., 2000. Evidence for natural fire and climate history since 37 ka BP in the northern part of the south China Sea. Sci. China (ser. D) 43, 487–493.

Sun, Y., Clemens, S.C., An, Z., Yu, Z., 2006. Astronomical timescale and palaeoclimatic implication of stacked 3.6-Myr monsoon records from the Chinese Loess Plateau. Quaternary Science Reviews 25, 33–48.

Sun, A.Z., Feng, Z.D., Ma, Y.Z., 2010. Vegetation and environmental changes in western Chinese Loess Plateau since 13.0 ka BP. Journal of Geographical Sciences 20, 177–192.

Swetnam, T.W., 1993. Fire history and climate change in giant sequoia groves. Science 262, 885–889.

Tan, Z.H., Huang, C.C., Pang, J.L., Li, P.H., 2005. Relationship between soil charcoal in Holocene and wildfire in the Zhouyuan region. Chinese Journal of Eco-Agriculture 13, 31–33 (in Chinese with English abstract).

Tang, L.Y., Li, C.H., An, C.B., Wang, W.G., 2007. Vegetation history of the western Loess Plateau of China during the last 40 ka based on pollen record. Acta Palaeontologia Sinica 46 (1), 45–61 (in Chinese with English abstract).

Thevenon, F., Williamson, D., Bard, E., Anselmetti, F.S., Beaufort, L., Cachier, H., 2010. Combining charcoal and elemental black carbon analysis in sedimentary archives: implications for past fire regimes, the pyrogenic carbon cycle, and the human–climate interactions. Global and Planetary Change 72, 381–389.

U.S. Climate Change Science Program, 2008. Synthesis and Assessment Product 4.3. The Effects of Climate Change on Agriculture, Land Resources, Water Resources, and Biodiversity. U.S. Department of Agriculture, Washington, DC, USA. (362 pp.).

Van der Werf, G.R., Randerson, J.T., Giglio, L., Collatz, G.J., Kasibhatla, P.S., 2006. Inter-annual variability in global biomass burning emission from 1997 to 2004. Atmospheric Chemistry and Physics 6, 3423–3441.

Vannière, B., Power, M.J., Roberts, N., Tinner, W., Carrión, J., Magny, M., Bartlein, P., Colombaroli, D., Daniau, A.L., Finsinger, W., Gil-Romera, G., Kaltenrieder, P., Magri, D., Pini, R., Sadori, L., Turner, R., Valsecchi, V., Vescovi, E., 2011. Circum-Mediterranean fire activity and climate changes during the mid-Holocene environmental transition (8500–2500 cal. BP). The Holocene 21, 53–73.

Von Grafenstein, U., Erlenkeuser, H., Brauer, A., Jouzel, J., Johnsen, S.J., 1999. A mid-European decadal isotope-climate record from 15500 to 5000 years B.P. Science 284, 1654–1657.

Wang, X., Peng, P.A., Ding, Z.L., 2005. Black carbon records in Chinese Loess Plateau over the last two glacial cycles and the implications for paleofires. Palaeogeography, Palaeoclimatology, Palaeoecology 223, 9–19.

Wang, Y.J., Cheng, H., Edwards, R.L., Kong, X.G., Shao, X.H., Chen, S.T., Wu, J.Y., Jiang, X.Y., Wang, X.F., An, Z.S., 2008. Millennial- and orbital-scale changes in the East Asian monsoon over the past 224,000 years. Nature 451, 1090–1093.

Westerling, A.L., Hidalgo, H.G., Cayan, D.R., Swetnam, T.W., 2006. Warming and earlier spring increase western US forest wildfire activity. Science 313, 940–943.

Whitlock, C., Bartlein, P.J., 2004. Holocene fire activity as a record of past environmental change. In: Gillespie, A., Porter, S.C., Atwater, B. (Eds.), The Quaternary period in the United States. 2003 INQUA Volume. Elsevier, pp. 479–489.

Whitlock, C., Millspaugh, S.H., 1996. Testing assumptions of fire history studies: an examination of modern charcoal accumulation in Yellowstone National Park. The Holocene 6, 7–15.

Whitlock, C., Shafer, S., Marlon, J., 2003a. The role of climate and vegetation change in shaping past and future fire regimes in the northwestern U.S. and the implications for ecosystem management. Forest Ecology and Management 178, 5–21.

Whitlock, C., Bartlein, P., Marlon, J., Brunelle, A., Long, C., 2003b. Holocene fire reconstructions from the northwestern U.S.: an examination at multiple time scales. 5th Symposium on Fire and Forest Meteorology, and 2nd International Wildland Fire Ecology and Fire Management Congress. American Meteorological Society, 16–20 November 2003, Orlando.

Whitlock, C., Skinner, C.N., Bartlein, P.J., Minckley, T., Mohr, J.A., 2004. Comparison of charcoal and tree-ring records of recent fires in the eastern Klamath Mountains, California, USA. Canadian Journal of Forest Research 34, 2110–2121.

Whitlock, C., Bianchi, M.M., Bartlein, P.J., Markgraf, V., Walsh, M., Marlon, J.M., McCoy, N., 2006. Postglacial vegetation, climate, and fire history along the east side of the Andes (lat 41–42.5 S), Argentina. Quaternary Research 66, 187–201.

Whitlock, C., Marlon, J., Briles, C., Brunelle, A., Long, C., Bartlein, P.J., 2008. Long-term relations among fire, fuel, and climate in the north-western US based on lake-sediment studies. International Journal of Wildland Fire 17, 72–83.

Xiao, J.L., Porter, S.C., An, Z.S., Kumai, H., Yoshikawa, S., 1995. Grain size of quartz as an indicator of winter monsoon strength on the Loess Plateau of central China during the last 130,000 yr. Quaternary Research 43, 22–29.

Yang, S.L., Ding, Z.L., 2004. Comparison of particle size characteristics of the Tertiary 'red clay' and Pleistocene loess in the Chinese Loess Plateau: implications for origin and sources of the 'red clay'. Sedimentology 51, 77–93.

Yang, S.L., Ding, Z.L., 2008. Advance–retreat history of the East-Asian summer monsoon rainfall belt over northern China during the last two glacial–interglacial cycles. Earth and Planetary Science Letters 274, 499–510.

Yang, Y., Shen, C.D., Yi, W.X., Sun, Y.M., Liu, T.S., 2001. The elemental carbon record in Weinan loess section since last 21 ka. Chinese Science Bulletin 46, 1541–1544.

Yu, Z.W., Ding, Z.L., 1998. An automatic orbital tuning method for paleoclimate records. Geophysical Research Letters 25, 4525–4528.

Zhang, W.X., Hu, S.X., 1989. The age and forming process of heilu soil in 'yuan' area of the east of Gansu province. Chinese Science Bulletin 16, 1252–1255.

Zhang, J.H., Wang, X.J., Qian, Y.H., Pei, S.Y., 2007. Environmental factor analysis of grass-land fire in Qinghai Province. Journal of Natural Disasters 16, 71–75 (in Chinese with English abstract).

Zhou, W.J., Donahue, D.J., Porter, S.C., Jull, A.J.T., Li, X.Q., Stuiver, M., An, Z.S., Matsumoto, E., Dong, G.R., 1996. Variability of monsoon climate in east Asia at the end of the last glaciation. Quaternary Research 46, 219–229.

Zhou, W.J., Head, M.J., Lu, X.F., An, Z.S., Jull, A.J.T., Donahue, D., 1999. Teleconnection of climatic events between East Asia and polar, high latitude areas during the last deglaciation. Palaeogeography, Palaeoclimatology, Palaeoecology 152, 163–172.

Zhou, W.J., Head, M.J., An, Z.S., Deckker, P.D., Liu, Z.Y., Liu, X.D., Lu, X.F., Jull, A.J.T., Donahue, D., 2001. Terrestrial evidence for a spatial structure of tropical–polar interconnections during the Younger Dryas episode. Earth and Planetary Science Letters 191, 231–239.

Zhou, W.J., Dodson, J., Head, M.J., L., B.S., Hou, Y.J., Lu, X.F., Donahue, D.J., Jull, A.J.T., 2002. Environmental variability within the Chinese desert–loess transition zone over the last 20000 years. The Holocene 12, 107–112.

Zolitzschka, B., Brauer, A., Negendank, J.F.W., Stockhausen, H., Lang, A., 2000. Annually dated late Weichselian continental paleoclimate record from the Eifel, Germany. Geology 28, 783–786.